Pharmacological Research 146 (2019) 104297

Contents lists available at ScienceDirect

Pharmacological Research

journal homepage: www.elsevier.com/locate/yphrs

Brain accumulation of osimertinib and its active metabolite AZ5104 is restricted by ABCB1 (P-glycoprotein) and ABCG2 (breast cancer resistance protein)

Stéphanie van Hoppe[a], Amer Jamalpoor[a], Johannes J.M. Rood[b], Els Wagenaar[a], Rolf W. Sparidans[b], Jos H. Beijnen[a,b], Alfred H. Schinkel[a,*]

[a] Division of Pharmacology, The Netherlands Cancer Institute, 1066 CX Amsterdam, The Netherlands
[b] Section of Pharmacoepidemiology & Clinical Pharmacology, Department of Pharmaceutical Sciences, Faculty of Science, Utrecht University, 3512 JE Utrecht, The Netherlands

ARTICLE INFO

Keywords:
ABCB1
ABCG2
Osimertinib
Brain accumulation
Oral availability
Tyrosine kinase inhibitor

ABSTRACT

Osimertinib is an irreversible EGFR inhibitor registered for advanced NSCLC patients whose tumors harbor recurrent somatic activating mutations in EGFR (EGFRm$^+$) or the frequently occurring EGFR-T790M resistance mutation. Using *in vitro* transport assays and appropriate knockout and transgenic mouse models, we investigated whether the multidrug efflux transporters ABCB1 and ABCG2 transport osimertinib and whether they influence the oral availability and brain accumulation of osimertinib and its most active metabolite, AZ5104. *In vitro*, human ABCB1 and mouse Abcg2 modestly transported osimertinib. In mice, Abcb1a/1b, with a minor contribution of Abcg2, markedly limited the brain accumulation of osimertinib and AZ5104. However, no effect of the ABC transporters was seen on osimertinib oral availability. In spite of up to 6-fold higher brain accumulation, we observed no acute toxicity signs of oral osimertinib in Abcb1a/1b;Abcg2 knockout mice. Interestingly, even in wild-type mice the intrinsic brain penetration of osimertinib was already relatively high, which may help to explain the documented partial efficacy of this drug against brain metastases. No substantial effects of mouse Cyp3a knockout or transgenic human CYP3A4 overexpression on oral osimertinib pharmacokinetics were observed, presumably due to a dominant role of mouse Cyp2d enzymes in osimertinib metabolism. Our results suggest that pharmacological inhibition of ABCB1 and ABCG2 during osimertinib therapy might potentially be considered to further benefit patients with brain (micro-)metastases positioned behind an intact blood-brain barrier, or with substantial expression of these transporters in the tumor cells, without invoking a high toxicity risk.

1. Introduction

Non-small cell lung cancer (NSCLC) is one of the leading causes of cancer death in the world, and it accounts for approximately 85% of all lung cancer diagnoses [1]. Advanced stage (IV) NSCLC is known to metastasize to a number of organs including the brain [2–6]. The identification of epidermal growth factor receptor (EGFR) mutations as one of the driving factors in NSCLC allowed the development of targeted therapy for NSCLC patients. EGFR-targeting tyrosine kinase inhibitors (TKIs) like gefitinib, erlotinib and several others display promising clinical activity in advanced NSCLC patients whose tumors harbor recurrent somatic activating mutations in EGFR (EGFRm$^+$) [7–12]. Unfortunately, although most of the EGFRm$^+$ NSCLC patients initially respond to these TKIs, there also is a high frequency of acquired resistance. The mechanism of acquired resistance for more than 50% of the patients is the acquisition of an additional EGFR mutation, EGFR-T790 M [13–15].

The search for novel therapeutic strategies targeted against this mutation has yielded a potent TKI, osimertinib (AZD9291, Tagrisso). Osimertinib covalently and irreversibly binds to cysteine 797 in the ATP binding site of EGFR, exhibiting 200 times greater potency toward both EGFRm$^+$ and T790M variants compared to the wild-type EGFR [16]. Osimertinib has been approved by the US FDA in April 2018 for the first-line treatment of metastatic NSCLC patients with epidermal growth factor (EGFR) exon 19 deletions or exon 21 L858R mutations in their tumors [17]. In clinical trials (phase II AURA), osimertinib has

* Corresponding author.
E-mail address: a.schinkel@nki.nl (A.H. Schinkel).

https://doi.org/10.1016/j.phrs.2019.104297
Received 1 April 2019; Received in revised form 21 May 2019; Accepted 4 June 2019
Available online 05 June 2019

demonstrated an overall objective response rate (ORR) of 62% and median progression-free survival (PFS) greater than 12 months with manageable toxicity. In patients with central nervous system (CNS) metastases the ORR for osimertinib was still 64%, but a shorter median PFS of 7 months was observed compared to patients without CNS metastases [18]. The absolute oral bioavailability of osimertinib is 69.8%, suggesting that it is well absorbed [19]. Additionally, previous reports have shown that osimertinib undergoes minimal first-pass metabolism with low clearance and is highly distributed to organs [19–21]. However, osimertinib is metabolized, mainly by cytochrome-P450 (CYP) 3A, into the active metabolites AZ5104 and AZ7550 (Supplemental Fig. 1), each amounting to ˜10% of the overall osimertinib systemic exposure. Interestingly, whereas AZ7550 showed a similar potency to osimertinib, AZ5104 showed greater potency than osimertinib against exon 19 deletion and T790 M mutants (˜8-fold) and wild-type (˜15-fold) EGFR [20,22].

Multidrug efflux transporters of the ATP-binding cassette (ABC) protein family can influence the disposition of a wide variety of endogenous and exogenous compounds, including many anti-cancer drugs. ABCB1 (P-glycoprotein) and ABCG2 (BCRP) occur in the apical membrane of epithelia in organs that are central to the absorption and elimination of drugs like kidney, liver, and small intestine. They are also found in blood-facing luminal membranes of barrier tissues protecting pharmacological sanctuary compartments like the blood-placenta, blood-testis, and blood–brain barriers (BBB). At these barriers ABCB1 and ABCG2 pump their substrates immediately out of the epithelial or endothelial cells back into the blood. Consequently, only limited amounts of drug can accumulate in, for instance, the brain to treat (micro) metastases that are located behind a functional BBB [23–25]. Many anticancer drugs including TKIs are transported by ABCB1, ABCG2, or both. These transporters can therefore significantly modulate the pharmacokinetics of these drugs, and hence their therapeutic efficacy and toxicity profile [26]. Several studies have shown that the oral availability of TKIs and their tissue (especially brain) penetration can be restricted due to interaction with ABCB1 and ABCG2 transporters [27–31]. Moreover, pharmacological inhibition of these ABC transporters can markedly enhance the brain accumulation of these drugs (*e.g.*, [27–31].

Some studies as well as the FDA documentation indicate that osimertinib can inhibit ABCB1 and ABCG2, and may possibly be transported by them [32–34]. If these transporters can also efficiently transport osimertinib *in vivo*, this might lead to decreased accumulation of osimertinib in transporter-expressing cancer cells, and thus tumor pharmacokinetic resistance. A recent study using an ABCB1-overexpressing multidrug-resistant KBv200 cell xenograft model in nude mice suggested that osimertinib-mediated inhibition of ABCB1 could enhance the tumor response against other ABCB1-transported drugs [34]. Moreover, NSCLC can metastasize to other parts of the body, including the brain. Upon initial diagnosis of NSCLC, brain metastases are observed in 20% of patients, with numbers increasing to 40–50% in those with stage III lung adenocarcinoma [4,6]. The brain is also a common site for disease relapse in patients previously treated with TKIs in about 30–60% of EGFR-mutated NSCLCs [5]. Osimertinib could potentially be a more successful candidate drug for these patients, as it is better targeted against these mutations. However, given the high ABCB1 and ABCG2 expression in the BBB, these transporters could potentially limit brain accumulation of osimertinib, which might reduce therapeutic efficiency against NSCLC CNS metastases.

In this study we therefore investigated whether osimertinib is transported by ABCB1 and ABCG2 *in vitro* or in mouse models, and how this might affect its oral plasma pharmacokinetics and brain penetration. We additionally studied the *in vivo* distribution of AZ5104. Furthermore, since osimertinib appears to be predominantly metabolized by human CYP3A4 [35,36], we also studied the influence of CYP3A on the oral systemic availability and tissue exposure of osimertinib.

2. Materials and methods

2.1. Chemicals

Osimertinib and zosuquidar were purchased from Sequoia Research Products (Pangbourne, U.K.), and Ko143 was obtained from Tocris Bioscience (Bristol, U.K.). GlutaMAX™ Dulbecco's Modified Eagle Medium (DMEM) and Dulbecco's phosphate buffered saline (PBS) were purchased from Gibco® by Life Technologies™ (The Netherlands). Glucose water 5% w/v was acquired from B. Braun Medical Supplies, Inc. (Melsungen, Germany). Bovine serum albumin (BSA) Fraction V was obtained from Roche Diagnostics (Mannheim, Germany). Isoflurane was purchased from Pharmachemie (Haarlem, The Netherlands), heparin (5000 IU ml^{-1}) was from Leo Pharma (Breda, The Netherlands). All other chemicals were acquired from Sigma-Aldrich (Steinheim, Germany) unless stated otherwise.

2.2. Transport assays

Polarized Madin-Darby canine kidney (MDCK-II) cell lines transduced with either human (h)ABCB1, hABCG2 or murine (m)Abcg2 cDNA were used and cultured as described previously [37]. Transepithelial transport assays were performed in triplicate on 12-well microporous polycarbonate membrane filters (3.0 µm pore size, Transwell 3402, Corning, Lowell, MA), as described [37]. In brief, cells were allowed to grow to an intact monolayer over 3 days, which was monitored with transepithelial electrical resistance (TEER; Millipore, USA) measurements. For all cell lines TEERs had to be above 80 O.cm^2 before the start of the transport experiment, and should not have decreased when re-measured after 8 h at the end of the experiment. On the third day, cells were washed with phosphate-buffered saline and pre-incubated with fresh DMEM medium including 10% fetal bovine serum and the relevant transport inhibitors for 1 h, where 5 µM zosuquidar (ABCB1 inhibitor) and/or 5 µM Ko143 (ABCG2/Abcg2 inhibitor) were added to both apical and basolateral compartments. To inhibit endogenous canine ABCB1 when testing the MDCK-II-mAbcg2 and MDCK-II-hABCG2 cell lines, we added 5 µM zosuquidar (ABCB1 inhibitor) to the culture medium throughout the experiment. The transport experiment was initiated by replacing the pre-incubation medium from the donor compartment (either basolateral or apical) with freshly prepared medium containing 2 µM osimertinib alone or in combination with the appropriate inhibitors. Plates were kept at 37 °C in 5% CO2 and 50 µl aliquots were taken from the acceptor compartment at 1, 2, 4 and 8 h and stored at −30 °C until analysis. The total amount of drug transported to the acceptor compartment was calculated after correction for volume loss due to sampling at each time point. Active transport was expressed by the relative transport ratio (r), defined as the amount of apically directed transport divided by the amount of basolaterally directed transport at the 8 h time point.

2.3. Animals

Male wild-type (WT) FVB, Abcb1a/1b$^{-/-}$ [38], Abcg2$^{-/-}$ [39], Abcb1a/1b;Abcg2$^{-/-}$ [40], Cyp3a$^{-/-}$ and Cyp3aXAV [41] mice of identical genetic background (> 99% FVB) were used. Groups of 5–6 mice per strain, aged between 9–14 weeks, were used. Animals were kept in a temperature-controlled environment with a 12 h light/dark cycle and received a standard diet (Transbreed, SDS Diets, Technilab-BMI, Someren, The Netherlands) and acidified water *ad libitum*. Mice were housed and handled according to institutional guidelines in compliance with Dutch and EU legislation.

2.4. Drug solutions

Osimertinib was first dissolved in dimethyl sulfoxide (DMSO) at a concentration of 25 mg/mL and further diluted with a mixture of

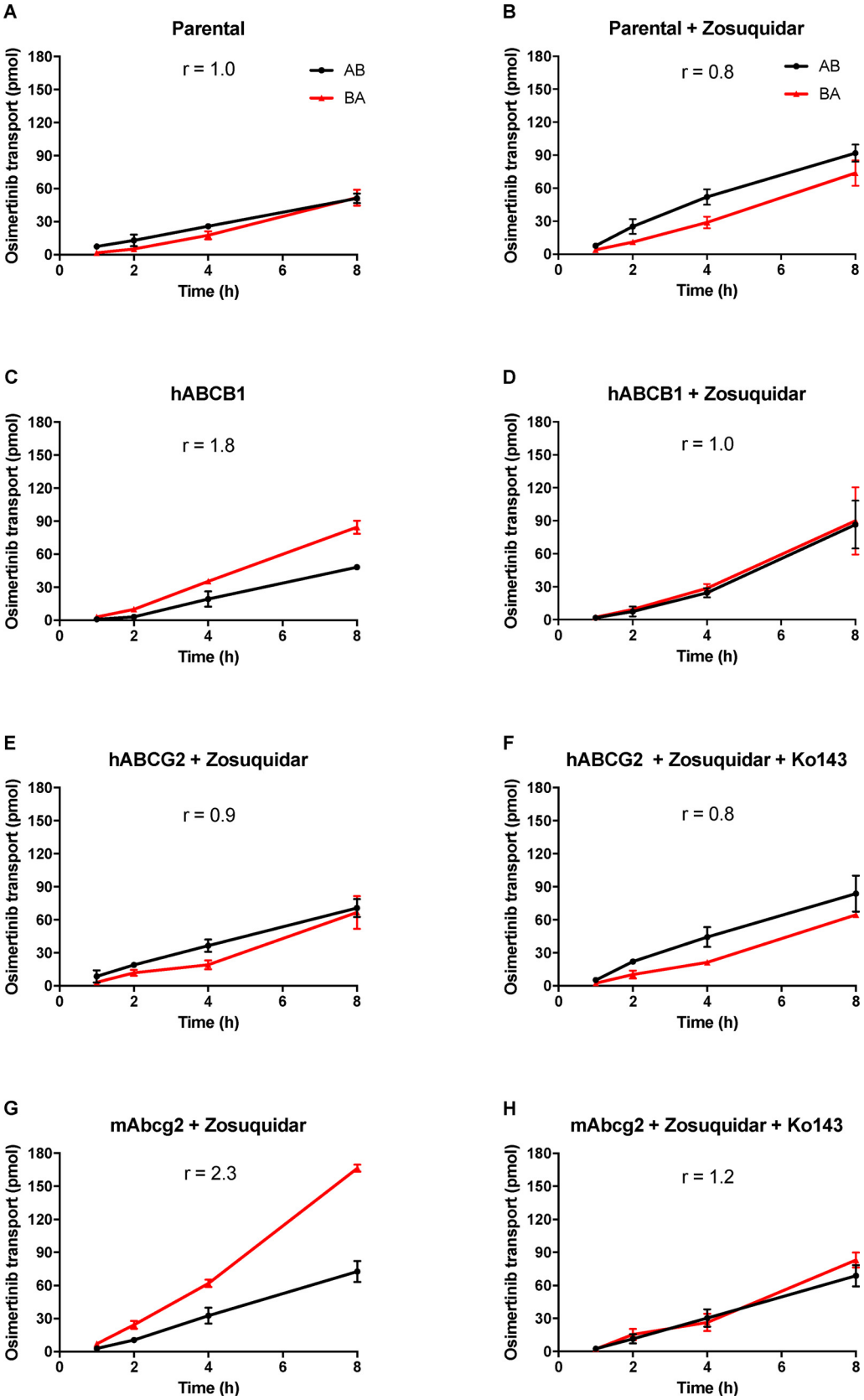

Fig. 1. *In vitro* transport of osimertinib. Transepithelial transport of osimertinib (2 μM) was assessed in MDCK-II cells either non-transduced (A, B) or transduced with hABCB1 (C, D), hABCG2 (E, F), or mAbcg2 (G, H) cDNA. At t = 0 h osimertinib was added to the donor compartment; thereafter at t = 1, 2, 4 and 8 h osimertinib concentrations were measured and plotted as total amount (pmol) of translocated drug (n = 3). (B, D-H) Zosuquidar (5 μM) and/or Ko143 (5 μM) were added as indicated to inhibit hABCB1 or hABCG2 and mAbcg2, respectively. r, relative transport ratio at 8 h. BA (red triangles), translocation from the basolateral to the apical compartment; AB (black circles), translocation from the apical to the basolateral compartment. Data are presented as mean ± SD. (For interpretation of the references to colour in this figure legend, the reader is referred to the web version of this article).

polysorbate 80: ethanol (1:1 v/v), and 5% w/v glucose water to yield a 1 mg/mL working solution. Final concentrations (v/v) of DMSO, polysorbate 80, ethanol, and glucose water were therefore 4%, 2.5%, 2.5% and 91%, respectively. Osimertinib was administered orally at a dose of 10 mg/kg body weight (10 μL/g).

2.5. Plasma and tissue pharmacokinetics of osimertinib and AZ5104

To minimize variation in absorption, mice were fasted for about 3 h prior to the oral administration of osimertinib using a blunt-ended needle. Fifty μL blood samples were drawn from the tail vein using heparin-coated capillaries (Sarstedt, Germany). At the last time point, mice were anesthetized using isoflurane inhalation, and blood was collected *via* cardiac puncture. For the 24 h experiment, tail vein sampling took place at 0.5, 1, 2, 4 and 8 h after oral administration; for the 1.5 h experiment, tail vein sampling took place at 5, 10, 15, 30 and 60 min after oral administration. At the end point, mice were sacrificed by cervical dislocation and a set of organs was rapidly removed, weighed, and subsequently frozen as whole organs at −30 °C. Organs were allowed to thaw on ice and homogenized in appropriate volumes of 4% (w/v) BSA in water using a FastPrep-24 device (MP Biomedicals, SA, California, USA). Homogenates were stored at −30 °C until analysis. Blood samples were immediately centrifuged at 9000 × *g* for 6 min at 4 °C, and plasma was collected and stored at −30 °C until analysis.

2.6. Drug analysis

Osimertinib concentrations in culture medium, plasma, and tissue homogenates were analyzed with a previously reported liquid-chromatography tandem mass spectrometric (LC–MS/MS) assay [42]. A new bioanalytical assay using LC–MS/MS was developed for simultaneous quantification of osimertinib (*m/z* 501.2 à 72.1) and the active desmethyl metabolite AZ5104 (*m/z* 487.2 à 72.1) based on our previously developed assay for only osimertinib [42]. Sample preparation was done by a simple protein crash with acetonitrile containing the stable isotopically labeled osimertinib ([13C2H3], *m/z* 505.2- > 72.1) as the internal standard. After partial evaporation of solvents and reconstitution in eluent the analytes were injected for quantification. The assay was successfully validated in a 2–2000 nM calibration range for both compounds. The Q1 *m/z* values for osimertinib, AZ5104 and 13C2H3-osimertinib were shifted +1 to the 13C-isotopes (*m/z* 501.2, 487.2, and 505.2) to avoid detector saturation, and thus improve linearity, of the QTRAP® 5500 triple quadrupole mass spectrometric detector (Sciex, Ontario, Canada).

2.7. Statistical and pharmacokinetic calculations

The area under the curve (AUC) of the plasma concentration-time data was calculated using the trapezoidal rule, without extrapolating to infinity using GraphPad Prism software 7.0e (GraphPad Software Inc., La Jolla, CA, USA). The maximum drug concentration in plasma (Cmax) and the time to reach maximum drug concentration in plasma (Tmax) were determined directly from individual concentration-time data. Tissue accumulation of osimertinib was calculated by determining the osimertinib tissue concentration relative to its plasma AUC from 0 to 24 h or 0–1.5 h. Average tissue to plasma ratios were calculated from individual mouse data. Statistical differences between individual groups were assessed using one-way analysis of variance (ANOVA) followed by Tukey's post-hoc multiple comparisons using GraphPad Prism. When variances were not homogeneously distributed, data were log-transformed before statistical tests were applied. A P value of < 0.05 was considered statistically significant. Data are presented as mean ± SD, with each experimental group containing 5–6 mice.

3. Results

3.1. Osimertinib is modestly transported by hABCB1 and mAbcg2 in vitro

We first studied the transport of osimertinib (2 μM) *in vitro* by measuring translocation through polarized monolayers of MDCK-II cell lines transduced with human (h)ABCB1, hABCG2 or mouse (m)Abcg2 cDNA. As shown in Fig. 1A, inthe parental line, both apically and basolaterally directed translocation of osimertinib were identical (efflux transport ratio $r = 1.0$). This r was somewhat, but not significantly, decreased when adding the ABCB1 inhibitor zosuquidar (Fig. 1B). In hABCB1-overexpressing MDCK-II cells, osimertinib was modestly transported in the apical direction ($r = 1.8$, Fig. 1C), and this transport was completely blocked by zosuquidar ($r = 1.0$, Fig. 1D). To suppress any possible endogenous canine ABCB1 transport activity, zosuquidar was added in subsequent experiments with MDCK-II cells overexpressing hABCG2 and mAbcg2. No significant active transport of osimertinib by hABCG2 was observed, and accordingly, addition of the hABCG2/mAbcg2 inhibitor Ko143 had little effect on overall translocation (Fig. 1E and 1 F). In contrast, in mAbcg2-overexpressing cells, clear apically directed transport of osimertinib was observed ($r = 2.3$), and this transport was completely abrogated by the addition of Ko143 (Fig. 1G and 1 H). Osimertinib thus appears to be modestly transported by hABCB1 and more efficiently by mAbcg2, but not detectably by hABCG2 *in vitro*. It is worth noting, however, that the effective dimeric transporter level per cell is somewhat lower in MDCKII-hABCG2 cells than in MDCKII-hABCB1 cells [43]. This comparatively low expression level might render a low level of osimertinib transport by hABCG2 undetectable.

3.2. No substantial effect of Abcb1 and Abcg2, or Cyp3a on plasma pharmacokinetics of oral osimertinib

In view of the *in vitro* transport results, we studied the impact of Abcb1 and Abcg2 on the plasma and tissue pharmacokinetics of osimertinib in a pilot experiment in male wild-type (WT) and Abcb1a/1b;Abcg2$^{-/-}$ mice. In addition, although metabolism of osimertinib in mice appears to be primarily mediated by mouse Cyp2d proteins and not by Cyp3a as in humans [44], we included Cyp3a$^{-/-}$ mice in this pilot. We orally administered osimertinib to the mice at a dosage of 10 mg/kg, physiologically roughly equivalent to the recommended human dose (80 mg oral, once daily). We analyzed the plasma concentrations of osimertinib over 24 h. As shown in Supplemental Fig. 2 and Table 1, we found a 1.4-fold higher plasma $AUC_{0\text{-}24h}$ in Abcb1a/1b;Abcg2$^{-/-}$ mice than in WT mice, but this was not statistically significant. Also the absence of Cyp3a enzymes did not cause a statistically significant shift compared to the WT mice in the plasma exposure between 0 and 24 h (Supplemental Fig. 2, Table 1).

We next assessed the tissue distribution of osimertinib at 24 h. As the plasma level of osimertinib at this time point was below the lower limit of detection in all strains, we could not directly calculate tissue-to-plasma ratios, but we could calculate the relative tissue accumulation (P) by correcting for the plasma $AUC_{0\text{-}24h}$. Interestingly, the tissue concentrations in brain but also liver of Abcb1a/1b;Abcg2$^{-/-}$ mice were markedly higher than those in WT or Cyp3a$^{-/-}$ mice, and this also applied when assessing the tissue accumulations (Table 1). By far the strongest effect was seen in brain. Although brain concentrations in WT mice were below the detection limit, and experimental variation was high, for instance the average brain concentration of osimertinib compared to that in liver was nearly 10-fold higher in Abcb1a/1b;Abcg2$^{-/-}$ mice (0.82) than in Cyp3a$^{-/-}$ mice (0.083). This parameter for other tissues such as spleen and kidney was much less affected (Supplemental Fig. 3). These data suggest that, at this late distribution phase, Abcb1a/1b and/or Abcg2 play a major role in limiting osimertinib concentrations in the brain, and a smaller role in limiting the concentrations in liver and spleen, in the latter cases perhaps by mediating late elimination from these organs (Table 1 and Supplemental Fig. 3). As for Cyp3a$^{-/-}$ mice, there were no tissue parameters significantly different from WT values at 24 h, but the C_{brain} and P_{brain} were markedly lower than in the Abcb1a/1b;Abcg2$^{-/-}$ mice (Table 1, Supplemental Fig. 3).

Table 1
Pharmacokinetic parameters of osimertinib over 24 h after oral administration of 10 mg/kg osimertinib to male WT, Abcb1a/1b;Abcg2$^{-/-}$ and Cyp3a$^{-/-}$ mice.

Parameter	Genotype		
	Wild-type	Abcb1a/1b;Abcg2$^{-/-}$	Cyp3a$^{-/-}$
Plasma AUC_{0-24} (h*ng/ml)	1833 ± 343	2639 ± 842	1418 ± 290
fold change	1.0	1.4	0.8
C_{max} (ng/ml)	272 ± 21	418 ± 167	341 ± 74
T_{max} (h)	1	1	1
C_{brain} (ng/g)	< 1	183 ± 145***	1.8 ± 1.0*/###
P_{brain} (*10^{-3} h^{-1})	< 1	70.8 ± 59.8***	1.4 ± 0.9*/###
C_{liver} (ng/g)	9.1 ± 8.4	223 ± 48***	21.6 ± 39.8###
fold change	1	24.4	2.4
P_{liver} (*10^{-3} h^{-1})	4.9 ± 5.1	87.0 ± 28.1***	3.0 ± 1.4###
fold change	1	17.7	0.6

AUC, area under the plasma concentration-time curve; C_{max}, maximum drug concentration in plasma; T_{max}, time (h) to reach maximum drug concentration in plasma; C_{tissue}, tissue concentration; P_{tissue}, tissue accumulation. The lower limit of quantification (LLoQ) value for osimertinib was set at 1 ng/ml. Osimertinib plasma concentrations in all the groups and brain concentrations in WT mice at 24 h were below the LLoQ. These values resulted occasionally in negative figures and were hence assumed to be zero for calculations. For statistical comparison the C_{brain} and P_{brain} values for WT mice (< 1) were assumed to be 1.0 ± 1.0. Statistical differences were assessed using one-way analysis of variance (ANOVA) followed by Tukey's post-hoc multiple comparisons. *, $P < 0.05$; **, $P < 0.01$; ***, $P < 0.001$ compared to WT mice. #, $P < 0.05$; ###, $P < 0.001$ compared to Abcb1a/1b;Abcg2$^{-/-}$ mice. Data are expressed as the mean ± SD. (n = 5–6).

3.3. Abcb1 and Abcg2 limit the brain accumulation of osimertinib

In all three tested mouse strains osimertinib reached its maximum plasma concentration approximately 1 h after oral administration (Supplemental Fig. 2). To better assess the separate and combined impact of Abcb1a/1b and Abcg2 on tissue distribution of osimertinib at, or shortly after, peak plasma exposure, we performed a 1.5 h pharmacokinetic experiment with oral administration of osimertinib (10 mg/kg) to male WT, Abcb1a/1b$^{-/-}$, Abcg2$^{-/-}$, and Abcb1a/1b;Abcg2$^{-/-}$ mice. Although, not unexpectedly, the interindividual variation this shortly after oral administration of osimertinib was high, the plasma AUCs of the four strains were very similar, with a C_{max} again occurring around 1 h (Fig. 2, Table 2). Only at the 90 min time point the Abcg2$^{-/-}$ plasma concentrations were significantly lower than those in the other strains, but this was probably related to the substantial experimental variation (Fig. 2). These results were generally in line with the 24 h data and suggest that the absence of Abcb1 and Abcg2, alone or combined, has no substantial effect on the plasma exposure of osimertinib in mice during the first hours after administration.

Similar to the results at 24 h after administration, the brain concentration of osimertinib in Abcb1a/1b;Abcg2$^{-/-}$ mice showed a highly significant, 5.1-fold increase ($P < 0.001$) compared to WT mice (Fig. 3A). Additionally, single Abcb1a/1b$^{-/-}$ mice displayed a statistically significant 3.5-fold increase ($P < 0.01$) compared to WT mice. In contrast, no significant difference was found between the single Abcg2$^{-/-}$ and WT mice. Correcting the osimertinib brain concentrations for the corresponding plasma concentrations (Fig. 3B) or plasma AUCs (Fig. 3C) yielded similar results. The brain-to-plasma ratios showed a highly significant, 6.4-fold increase ($P < 0.001$) for Abcb1a/1b;Abcg2$^{-/-}$ mice compared to WT mice, and a 4.1-fold increase for Abcb1a/1b$^{-/-}$ mice ($P < 0.05$), whereas values in the Abcg2$^{-/-}$ mice were not significantly different from those in the WT mice (Fig. 3B; Table 2). Analyzing the same parameters for the liver did not show significant differences between the strains (Fig. 3 D–F) except for the Abcg2$^{-/-}$ liver-to-plasma ratio, which was, however, determined only by

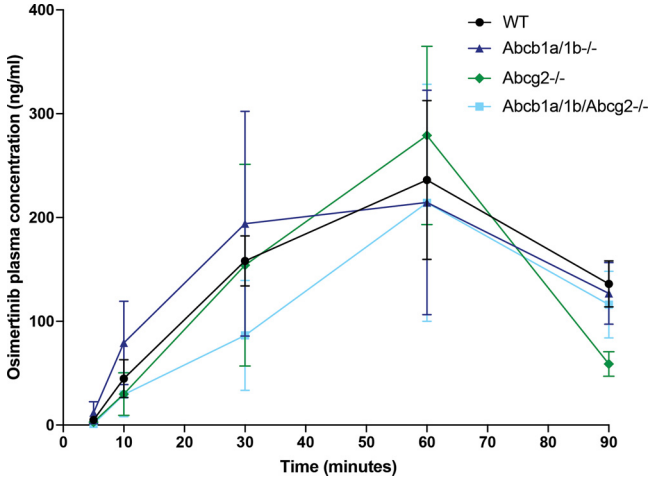

Fig. 2. Plasma concentration-time curves of osimertinib in male wild-type (WT) (black circles), Abcb1a/1b$^{-/-}$ (dark blue triangles), Abcg2$^{-/-}$ (green diamonds) and Abcb1a/1b;Abcg2$^{-/-}$ (light-blue squares) mice, over 90 min after oral administration of 10 mg/kg osimertinib. Data are given as mean ± SD. N = 5–6 mice per group. (For interpretation of the references to colour in this figure legend, the reader is referred to the web version of this article).

the unexpectedly low plasma concentration in this strain at the single 1.5 h time point (Fig. 2). Thus, also at 1.5 h, especially Abcb1a/1b could profoundly restrict the brain accumulation of osimertinib, and the combined deficiency for both transporters resulted in a further increased brain penetration of osimertinib. Strikingly, in the absence of Abcb1a/1b and/or Abcg2, the brain-to-plasma ratios of osimertinib (60 to 90) were even higher than the liver-to-plasma ratios (30 to 70), suggesting a high intrinsic capacity of osimertinib to accumulate in the brain as well as the liver (Fig. 3B and E). Indeed, even in WT mice the brain-to-plasma ratio of osimertinib was still relatively high (14.5, Fig. 3B, Table 2), illustrating the propensity of this drug to accumulate into the brain.

For some TKIs, such as brigatinib, we have previously observed that increased brain penetration of the drug due to the absence of Abcb1a/1b and Abcg2 activity at the BBB in mice was associated with acute lethal toxicity, whereas WT mice were completely unaffected by the same dose of brigatinib [45]. In contrast, in our current study for osimertinib we did not observe any indication for acute toxicity in the Abcb1a/1b;Abcg2$^{-/-}$ mice in either the 24-h or the 1.5-h experiments after a single 10 mg/kg oral dose.

3.4. Limited impact of mouse Cyp3a and human CYP3A4 on osimertinib pharmacokinetics in mice

Although the 24 h experiment did not suggest a clear impact of mouse Cyp3a on osimertinib plasma pharmacokinetics, we did assess a possible impact of Cyp3a deficiency, and/or the transgenic overexpression of human CYP3A4 in liver and intestine, on the plasma kinetics and tissue distribution of osimertinib 1.5 h after oral administration at 10 mg/kg to male mice. Fig. 4 and Supplemental Table 1 show that, unexpectedly, and in spite of the high interindividual variation, the plasma $AUC_{0-1.5h}$ was significantly lower in both the Cyp3a$^{-/-}$ and CYP3A4-transgenic mice compared to the WT strain. For the Cyp3a$^{-/-}$ mice this contrasts with the 24 h plasma data, and it may be that the high interindividual variation played a role in this result. A possible lowering of the plasma AUC in Cyp3a$^{-/-}$ mice might in theory be caused by compensatory upregulation of other osimertinib-clearing proteins. A possible slight (but significant, $P < 0.05$) further decrease in the plasma $AUC_{0-1.5h}$ in the CYP3A4-transgenic mice compared to the Cyp3a$^{-/-}$ mice (Supplemental Table 1) might suggest a comparatively small impact of the human CYP3A4 expression on osimertinib

Table 2
Pharmacokinetic parameters of osimertinib over 1.5 h after oral administration of 10 mg/kg osimertinib to male WT, Abcb1a/1b$^{-/-}$, Abcg2$^{-/-}$, and Abcb1a/1b;Abcg2$^{-/-}$ mice.

Parameter	Genotype			
	Wild-type	Abcb1a/1b$^{-/-}$	Abcg2$^{-/-}$	Abcb1a/1b;Abcg2$^{-/-}$
Plasma $AUC_{0\text{-}1.5}$ (h*ng/ml)	227 ± 50	236 ± 77	225 ± 71	178 ± 78
fold change	1	1	1	0.8
C_{max} (ng/ml)	236 ± 77	215 ± 108	279 ± 86	214 ± 114
T_{max} (h)	1	1	1	1
C_{brain} (ng/g)	2003 ± 1026	6929 ± 3161**	1350 ± 271	10135 ± 1942***
fold change	1	3.5	0.7	5.1
Brain to plasma ratio	14.5 ± 6.4	60.5 ± 36.7*	23.1 ± 3.7	93.0 ± 18.3***
fold change	1	4.1	1.6	6.4
P_{brain} (h^{-1})	8.6 ± 3.6	32.8 ± 20.6	6.5 ± 2.3	64.3 ± 22.8***
fold change	1	3.8	0.8	7.5
C_{liver}(ng/g)	3912 ± 1180	3934 ± 1842	3917 ± 362	2472 ± 494
fold change	1	1	1	0.6
Liver to plasma ratio	29.0 ± 9.2	33.4 ± 19.8	68.9 ± 16.8**	28.4 ± 14.2
fold change	1	1.2	2.4	1
P_{liver} (h^{-1})	17.3 ± 4.6	17.6 ± 9.4	18.6 ± 5.5	15.7 ± 5.7
fold change	1	1	1	0.9
Brain to liver ratio	0.6 ± 0.3	2.1 ± 1.5	0.3 ± 0.1	3.6 ± 1.1***
fold change	1	3.5	0.5	6

AUC, area under the plasma concentration-time curve; C_{max}, maximum drug concentration in plasma; T_{max}, time (h) to reach maximum drug concentration in plasma; C_{tissue}, tissue concentration; P_{tissue}, tissue accumulation. Statistical differences were assessed using one-way analysis of variance (ANOVA) followed by Tukey's post-hoc multiple comparisons. *, P < 0.05; **, P < 0.01; ***, P < 0.001 compared to WT mice. Data are expressed as the mean ± SD. (n = 5–6).

clearance. However, all these effects are very modest. Also, when considering the various tissue concentrations of osimertinib, values for the three strains for brain, liver, kidney, spleen, and testis were all relatively close and not significantly different (Supplemental Table 1 and data not shown). Overall, there is therefore no indication that Cyp3a or CYP3A4 activity has a major impact on the plasma exposure and tissue distribution of osimertinib in mice.

3.5. Brain accumulation of the active metabolite AZ5104 is restricted by Abcb1a/1b and Abcg2

In the final phase of this study an LC–MS/MS assay became available for the pharmacodynamically most active metabolite of osimertinib, AZ5104 (Supplemental Fig. 1). Samples still available from the 1.5 h study with ABC transporter knockout strains could then be re-measured for the presence of this compound after oral administration of osimertinib. As shown in Supplemental Fig. 4, the plasma

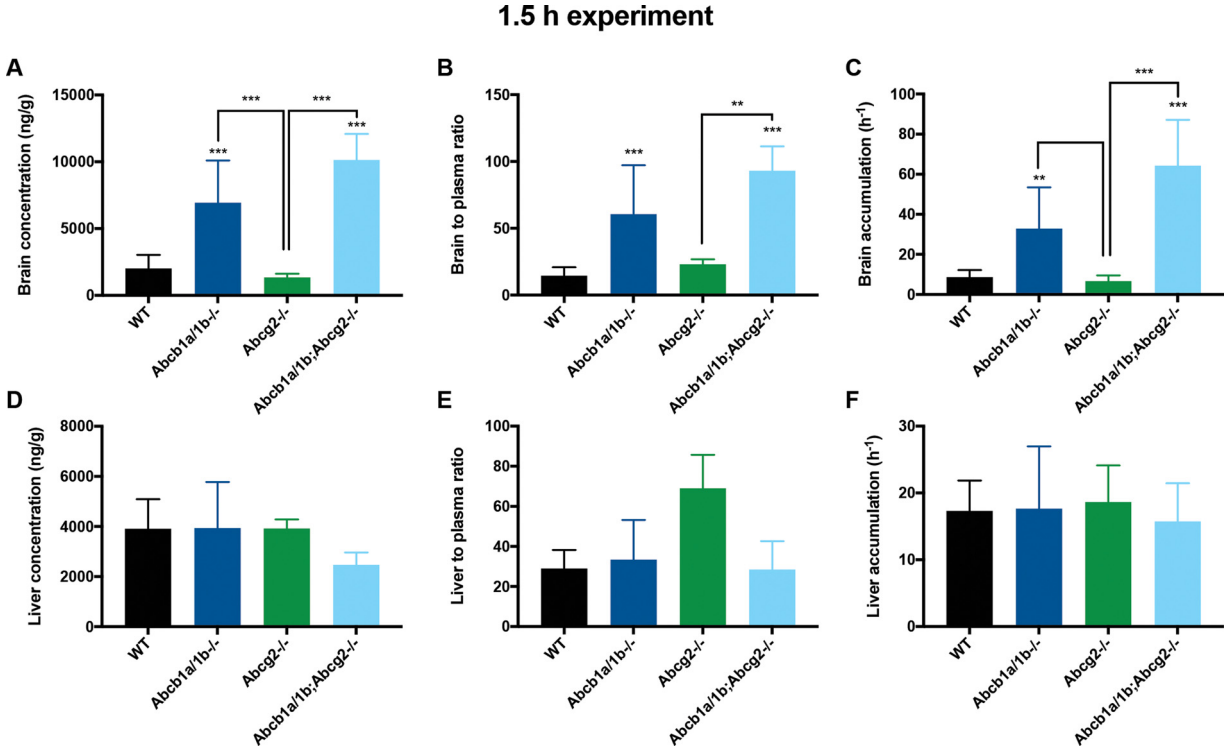

Fig. 3. Brain and liver concentration (A, D), tissue-to-plasma ratio (B, E) and relative tissue accumulation (C, F) of osimertinib in male WT, Abcb1a/1b$^{-/-}$, Abcg2$^{-/-}$, and Abcb1a/1b;Abcg2$^{-/-}$ mice 1.5 h after oral administration of 10 mg/kg osimertinib. *, P < 0.05; **, P < 0.01; ***, P < 0.001 compared to WT mice. Data are presented as the mean ± SD. N = 5 mice per group.

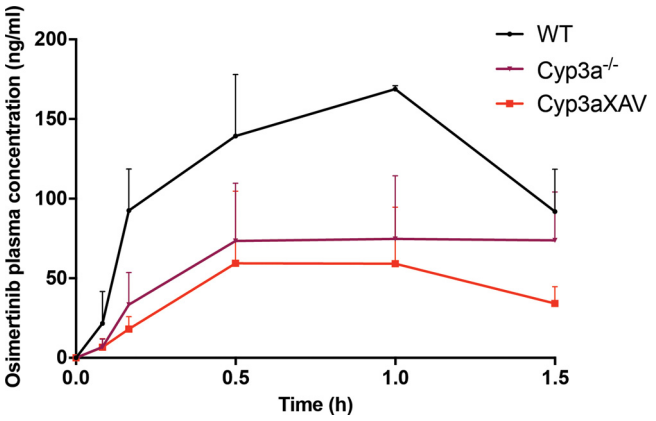

Fig. 4. Plasma concentration-time curves of osimertinib in male wild-type (WT) (black circles), Cyp3a$^{-/-}$ (purple triangles), Cyp3aXAV (red squares) mice, over 90 min after oral administration of 10 mg/kg osimertinib. Data are given as mean ± SD. N = 5–6 mice per group. (For interpretation of the references to colour in this figure legend, the reader is referred to the web version of this article).

concentrations of AZ5104 and the AZ5104-to-osimertinib ratios gradually rose between 0.5 and 1.5 h, with no significant differences between the four tested strains (WT, Abcb1a/1b$^{-/-}$, Abcg2$^{-/-}$, and Abcb1a/1b;Abcg2$^{-/-}$). The metabolite-to-osimertinib ratio was about 20–25% at 1.5 h. Whereas the plasma levels of AZ5104 were thus hardly affected by the ABC transporters, its brain concentration, brain-to-plasma ratio, and brain accumulation were dramatically increased in the Abcb1a/1b$^{-/-}$ mice, but especially in the Abcb1a/1b;Abcg2$^{-/-}$ mice (Fig. 5A-C). Abcg2 deficiency did not show a significant difference compared to WT mice. However, the significant difference between Abcb1a/1b and Abcb1a/1b;Abcg2$^{-/-}$ mice in the brain ($P < 0.001$) does suggest that Abcg2 plays an important role in AZ5104 transport across the BBB. At the same time, the equivalent parameters for AZ5104 in the liver were not significantly altered between the strains (Fig. 5D–F). It thus appears that Abcb1a/1b and to a lesser extent also Abcg2 at the BBB can strongly restrict the brain accumulation of AZ5104.

4. Discussion

ABC efflux transporters, especially ABCB1 and ABCG2, have been shown to be associated with resistance to chemotherapy in several cancer cell lines, including NSCLC [25,46]. Furthermore, brain metastases are a common occurrence in patients suffering from NSCLC [4–6,47]. Because ABCB1 and ABCG2 are expressed at the BBB, these transporter proteins may play a significant role in limiting the pharmacotherapeutic treatment of cancer metastases in the brain. Given the recent therapeutic success of osimertinib in NSCLC patients, we wanted to investigate the possible effects of these transporters on osimertinib disposition.

Our results show that osimertinib is transported by hABCB1 and efficiently by mAbcg2, but not detectably by hABCG2 *in vitro*, and that this transport can be inhibited with specific inhibitors. A previous report demonstrated that osimertinib at low concentration (00.4 μM) can also significantly reverse hABCB1 and hABCG2 mediated multidrug resistance (MDR) *via* inhibiting their efflux activity *in vitro* [34], illustrating the various interactions of osimertinib with these transporters.

In spite of the clear transport *in vitro*, *in vivo* we did not observe an obvious limiting effect of Abcb1a/1b or Abcg2 on the oral availability of osimertinib in mice. However, the accumulation of osimertinib in the

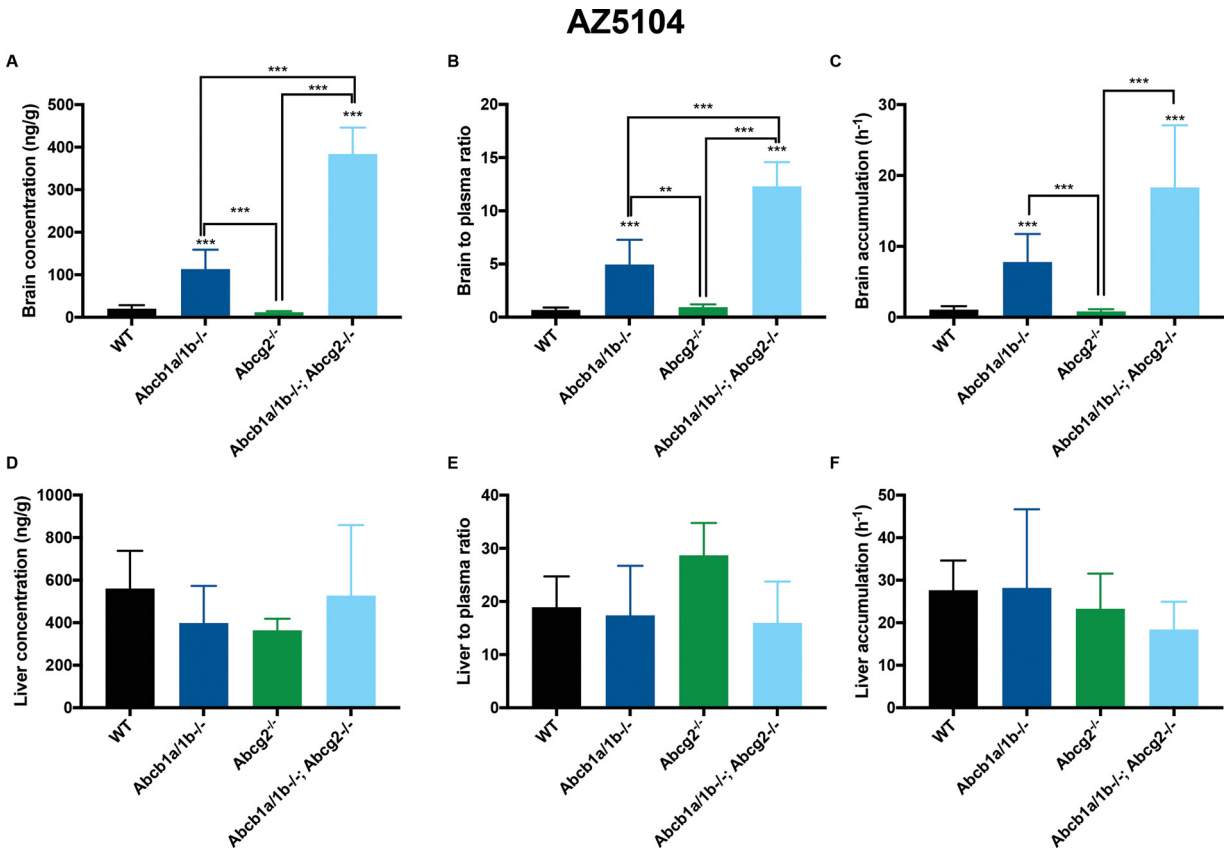

Fig. 5. Brain and liver concentration (A, D), tissue-to-plasma ratio (B, E) and relative tissue accumulation (C, F) of AZ5104 in male WT, Abcb1a/1b$^{-/-}$, Abcg2$^{-/-}$, and Abcb1a/1b;Abcg2$^{-/-}$ mice 1.5 h after oral administration of 10 mg/kg osimertinib. *, $P < 0.05$; **, $P < 0.01$; ***, $P < 0.001$ compared to WT mice. Data are presented as the mean ± SD. N = 5 mice per group.

brain was markedly restricted by Abcb1a/1b and Abcg2. The brain distribution of osimertinib was clearly increased by absence of the combination of Abcb1a/1b and Abcg2 in the BBB (6.4-fold compared to WT), but not substantially by absence of Abcg2 alone. This is in contrast to Abcb1a/1b, which by itself showed a clear limiting effect (by 4.1-fold) on osimertinib accumulation in the brain (Fig. 3, Table 2). These data suggest that the brain penetration of osimertinib could be further enhanced by effectively inhibiting ABCB1 and ABCG activity in the BBB, for instance by coadministration of the dual ABCB1 and ABCG2 inhibitor elacridar with osimertinib.

In this context it is worth noting that we did not observe any indication that the increased brain penetration of osimertinib in Abcb1a/1b;Abcg2$^{-/-}$ mice resulted in noticeable toxicity. This is in contrast to the TKI brigatinib, which caused lethal toxicity in Abcb1a/1b;Abcg2$^{-/-}$ mice, whereas WT mice were completely unaffected by the same oral dose of brigatinib [45]. This suggests that it may potentially be safe enough to boost osimertinib brain accumulation using ABCB1 and ABCG2 inhibitors, although obviously this will always first need to be carefully tested in appropriately designed clinical trials.

The brain penetration of the most active metabolite of osimertinib, AZ5104, was also strongly limited by Abcb1a/1b activity in the BBB, and more notably so when Abcg2 was additionally deficient (Fig. 5). This suggests that AZ5104 is similarly affected by the ABC transporters at the BBB as its parental compound. In contrast, the distribution of osimertinib and AZ5104 to the liver was not markedly affected by these efflux transporters (Figs. 3 and 5).

The difference we observed between a high impact on brain accumulation *versus* no significant impact on oral availability of osimertinib is a common observation for various other shared Abcb1a/1b and Abcg2 substrates such as sunitinib, sorafenib, imatinib, and gefitinib [27,48–50]. We have observed that when a drug is only modestly transported by ABCB1 and/or ABCG2 *in vitro*, we generally see a much more outspoken effect of these transporters in limiting the brain accumulation of this drug, than in reducing its oral availability [51,52]. Only drugs that are very efficiently transported *in vitro*, like afatinib, tend to show a clear role of the transporters in restricting their oral availability [53]. We suspect that this could be due to a much more abundant presence of various other drug uptake systems as well as an overall higher influx capacity in the intestine as compared to the BBB. Thus, when removing or inhibiting ABCB1 and/or ABCG2, the oral availability of a substrate drug will generally be less enhanced than its brain penetration.

In humans, osimertinib is thought to be predominantly metabolized by the CYP3A4/5 enzymes, while in mice this appears to be primarily mediated by mouse Cyp2d proteins [44]. We observed no significant impact of Cyp3a deficiency on the osimertinib systemic availability and its tissue exposure. This is consistent with a study showing that co-dosing mice with osimertinib and the CYP450 inhibitor benzotriazole-1-amine did not have a significant effect on osimertinib metabolism [54]. Also, we observed only a borderline significant difference in AUC between the Cyp3aXAV and Cyp3a$^{-/-}$ mice. These findings can probably be explained by a dominant function of the murine Cyp2d proteins in these mice [44].

Various clinical trials have assessed the therapeutic efficacy of osimertinib for NSCLC and metastatic NSCLC patients. A recent study demonstrated that patients treated with osimertinib developed CNS metastases to a lesser extent compared to the standard EGFR-TKIs treatment. In addition, another study showed that osimertinib had a reasonably high ORR in CNS metastases of 64% [18,55]. These findings clearly suggest the promising therapeutic efficiency osimertinib could offer for NSCLC patients both with and without CNS involvement. One factor as to why osimertinib seems to be partially effective against brain metastases could be its intrinsically high brain penetration. In fact, the brain-to-plasma ratio in WT mice (14.5, Fig. 3, Table 2) was only slightly lower than the liver-to-plasma ratio [29], and in Abcb1a/1b;Abcg2$^{-/-}$ mice it was even considerably higher (93.0 in brain *vs* 28.4 in liver). This already favorable behavior of osimertinib with respect to brain metastases might therefore possibly be even further boosted by coadministration of efficient ABCB1 and ABCG2 inhibitors.

Based on our findings, it is further likely that tumors substantially expressing ABCB1 and/or ABCG2 will also display some resistance to osimertinib-based chemotherapy. Thus, inhibiting these transporters with effective dual ABCB1 and ABCG2 inhibitors such as elacridar during osimertinib therapy could potentially further improve the tumor response. However, caution should always be exercised to prevent unexpected toxicities, and these possible approaches will first need to be carefully examined in clinical trials, as would also apply to efforts to increase osimertinib levels in the brain of patients with CNS tumors or metastases.

5. Conclusion

Our study shows that ABCB1 and ABCG2 do not restrict the oral availability of osimertinib, but that they do markedly restrict the brain disposition of both osimertinib and AZ5104. These results suggest that coadministration of ABCB1 and ABCG2 inhibitors may be an option to enhance osimertinib exposure in patients, especially in the brain. This could provide a better option to treat NSCLC and its metastases located in part or in whole behind a functional blood-brain barrier.

Conflict of interest

The research group of A.H.S. receives revenue from commercial distribution of some of the mouse strains used in this study.

Appendix A. Supplementary data

Supplementary material related to this article can be found, in the online version, at doi:https://doi.org/10.1016/j.phrs.2019.104297.

References

[1] M.A. Bareschino, C. Schettino, A. Rossi, et al., Treatment of advanced non small cell lung cancer, J. Thorac. Dis. 2 (2011) 122–133, https://doi.org/10.3978/j.issn.2072-1439.2010.12.08.
[2] R. Thippeswamy, V. Noronha, V. Krishna, et al., Stage IV lung cancer: is cure possible? Indian J. Med. Paediatr. Oncol. 2 (2013) 121–125, https://doi.org/10.4103/0971-5851.116207.
[3] L.E. Quint, S. Tummala, L.J. Brisson, et al., Distribution of distant metastases from newly diagnosed non-small cell lung cancer, Ann. Thorac. Surg. 1 (1996) 246–250.
[4] H.J. Mamon, B.Y. Yeap, P.A. Janne, et al., High risk of brain metastases in surgically staged IIIA non-small-cell lung cancer patients treated with surgery, chemotherapy, and radiation, J. Clin. Oncol. 7 (2005) 1530–1537, https://doi.org/10.1200/JCO.2005.04.123.
[5] S. Heon, B.Y. Yeap, G.J. Britt, et al., Development of central nervous system metastases in patients with advanced non-small cell lung cancer and somatic EGFR mutations treated with gefitinib or erlotinib, Clin. Cancer Res. 23 (2010) 5873–5882, https://doi.org/10.1158/1078-0432.CCR-10-1588.
[6] J.S. Barnholtz-Sloan, A.E. Sloan, F.G. Davis, et al., Incidence proportions of brain metastases in patients diagnosed (1973 to 2001) in the Metropolitan Detroit Cancer surveillance System, J. Clin. Oncol. 14 (2004) 2865–2872, https://doi.org/10.1200/JCO.2004.12.149.
[7] M. Maemondo, A. Inoue, K. Kobayashi, et al., Gefitinib or chemotherapy for non-small-cell lung cancer with mutated EGFR, N. Engl. J. Med. 25 (2010) 2380–2388, https://doi.org/10.1056/NEJMoa0909530.
[8] R. Rosell, E. Carcereny, R. Gervais, et al., Erlotinib versus standard chemotherapy as first-line treatment for European patients with advanced EGFR mutation-positive non-small-cell lung cancer (EURTAC): a multicentre, open-label, randomised phase 3 trial, Lancet Oncol. 3 (2012) 239–246, https://doi.org/10.1016/S1470-2045(11)70393-X.
[9] L.V. Sequist, J.C. Yang, N. Yamamoto, et al., Phase III study of afatinib or cisplatin plus pemetrexed in patients with metastatic lung adenocarcinoma with EGFR mutations, J. Clin. Oncol. 27 (2013) 3327–3334, https://doi.org/10.1200/JCO.2012.44.2806.
[10] S.S. Ramalingam, K. O'Byrne, M. Boyer, et al., Dacomitinib versus erlotinib in patients with EGFR-mutated advanced nonsmall-cell lung cancer (NSCLC): pooled subset analyses from two randomized trials, Ann. Oncol. 3 (2016) 423–429, https://doi.org/10.1093/annonc/mdv593.
[11] S. Rossi, L. Toschi, G. Finocchiaro, et al., Impact of Exon 19 deletion subtypes in EGFR-Mutant metastatic non-small-Cell lung Cancer Treated with first-line tyrosine kinase inhibitors, Clin. Lung Cancer (2018) 82–87, https://doi.org/10.1016/j.cllc.

2018.10.009.
[12] Y. Cai, X. Wang, Y. Guo, et al., Successful treatment of a lung adenocarcinoma patient with a novel EGFR exon 20-ins mutation with afatinib: A case report, Medicine (Baltimore) 1 (2019) e13890, https://doi.org/10.1097/MD.0000000000013890.
[13] W. Pao, V.A. Miller, K.A. Politi, et al., Acquired resistance of lung adenocarcinomas to gefitinib or erlotinib is associated with a second mutation in the EGFR kinase domain, PLoS Med. 3 (2005) e73, https://doi.org/10.1371/journal.pmed.0020073.
[14] D. Planchard, Y. Loriot, F. Andre, et al., EGFR-independent mechanisms of acquired resistance to AZD9291 in EGFR T790M-positive NSCLC patients, Ann. Oncol. 10 (2015) 2073–2078, https://doi.org/10.1093/annonc/mdv319.
[15] S. Kobayashi, T.J. Boggon, T. Dayaram, et al., EGFR mutation and resistance of non-small-cell lung cancer to gefitinib, N. Engl. J. Med. 8 (2005) 786–792, https://doi.org/10.1056/NEJMoa044238.
[16] D.A. Cross, S.E. Ashton, S. Ghiorghiu, et al., AZD9291, an irreversible EGFR TKI, overcomes T790M-mediated resistance to EGFR inhibitors in lung cancer, Cancer Discov. 9 (2014) 1046–1061, https://doi.org/10.1158/2159-8290.CD-14-0337.
[17] Center for Drug Valuation and Research of the U.S., Department of Health and Human Servics Food and Drug Administration, (2018) https://wwwfdagov/Drugs/InformationOnDrugs/ApprovedDrugs/ucm605113htm.
[18] J.C. Yang, M.J. Ahn, D.W. Kim, et al., Osimertinib in Pretreated T790M-Positive Advanced Non-Small-Cell Lung Cancer: AURA Study Phase II Extension Component, J. Clin. Oncol. 12 (2017) 1288–1296, https://doi.org/10.1200/JCO.2016.70.3223.
[19] K. Vishwanathan, K. So, K. Thomas, et al., Absolute Bioavailability of Osimertinib in Healthy Adults, Clin. Pharmacol. Drug Dev. 2 (2019) 198–207, https://doi.org/10.1002/cpdd.467.
[20] P.A. Dickinson, M.V. Cantarini, J. Collier, et al., Metabolic Disposition of Osimertinib in Rats, Dogs, and Humans: Insights into a Drug Designed to Bind Covalently to a Cysteine Residue of Epidermal Growth Factor Receptor, Drug Metab. Dispos. 8 (2016) 1201–1212, https://doi.org/10.1124/dmd.115.069203.
[21] D. Planchard, K.H. Brown, D.W. Kim, et al., Osimertinib Western and Asian clinical pharmacokinetics in patients and healthy volunteers: implications for formulation, dose, and dosing frequency in pivotal clinical studies, Cancer Chemother. Pharmacol. 4 (2016) 767–776, https://doi.org/10.1007/s00280-016-2992-z.
[22] Center for Drug Valuation and Research of the U.S., Department of Health and Human Servics Food and Drug Administration., HIGHLIGHTS OF PRESCRIBING INFORMATION, (2017).
[23] A.H. Schinkel, E. Wagenaar, C.A. Mol, et al., P-glycoprotein in the blood-brain barrier of mice influences the brain penetration and pharmacological activity of many drugs, J. Clin. Invest. 11 (1996) 2517–2524, https://doi.org/10.1172/JCI118699.
[24] M.L. Vlaming, J.S. Lagas, A.H. Schinkel, Physiological and pharmacological roles of ABCG2 (BCRP): recent findings in Abcg2 knockout mice, Adv. Drug Deliv. Rev. 1 (2009) 14–25, https://doi.org/10.1016/j.addr.2008.08.007.
[25] N. Yabuki, K. Sakata, T. Yamasaki, et al., Gene amplification and expression in lung cancer cells with acquired paclitaxel resistance, Cancer Genet. Cytogenet. 1 (2007) 1–9, https://doi.org/10.1016/j.cancergencyto.2006.07.020.
[26] F.E. Stuurman, B. Nuijen, J.H. Beijnen, et al., Oral anticancer drugs: mechanisms of low bioavailability and strategies for improvement, Clin. Pharmacokinet. 6 (2013) 399–414, https://doi.org/10.1007/s40262-013-0040-2.
[27] S.C. Tang, J.S. Lagas, N.A. Lankheet, et al., Brain accumulation of sunitinib is restricted by P-glycoprotein (ABCB1) and breast cancer resistance protein (ABCG2) and can be enhanced by oral elacridar and sunitinib coadministration, Int. J. Cancer 1 (2012) 223–233, https://doi.org/10.1002/ijc.26000.
[28] S.C. Tang, L.N. Nguyen, R.W. Sparidans, et al., Increased oral availability and brain accumulation of the ALK inhibitor crizotinib by coadministration of the P-glycoprotein (ABCB1) and breast cancer resistance protein (ABCG2) inhibitor elacridar, Int. J. Cancer 6 (2014) 1484–1494, https://doi.org/10.1002/ijc.28475.
[29] H. Kodaira, H. Kusuhara, J. Ushiki, et al., Kinetic analysis of the cooperation of P-glycoprotein (P-gp/Abcb1) and breast cancer resistance protein (Bcrp/Abcg2) in limiting the brain and testis penetration of erlotinib, flavopiridol, and mitoxantrone, J. Pharmacol. Exp. Ther. 3 (2010) 788–796, https://doi.org/10.1124/jpet.109.162321.
[30] S. Shukla, Z.S. Chen, S.V. Ambudkar, Tyrosine kinase inhibitors as modulators of ABC transporter-mediated drug resistance, Drug Resist. Updat. 1-2 (2012) 70–80, https://doi.org/10.1016/j.drup.2012.01.005.
[31] J.S. Lagas, R.A. van Waterschoot, V.A. van Tilburg, et al., Brain accumulation of dasatinib is restricted by P-glycoprotein (ABCB1) and breast cancer resistance protein (ABCG2) and can be enhanced by elacridar treatment, Clin. Cancer Res. 7 (2009) 2344–2351, https://doi.org/10.1158/1078-0432.ccr-08-2253.
[32] S.H. Hsiao, Y.J. Lu, Y.Q. Li, et al., Osimertinib (AZD9291) Attenuates the Function of Multidrug Resistance-Linked ATP-Binding Cassette Transporter ABCB1 in Vitro, Mol. Pharm. 6 (2016) 2117–2125, https://doi.org/10.1021/acs.molpharmaceut.6b00249.
[33] X.Y. Zhang, Y.K. Zhang, Y.J. Wang, et al., Osimertinib (AZD9291), a Mutant-Selective EGFR Inhibitor, Reverses ABCB1-Mediated Drug Resistance in Cancer Cells, Molecules 9 (2016), https://doi.org/10.3390/molecules21091236.
[34] Z. Chen, Y. Chen, M. Xu, et al., Osimertinib (AZD9291) Enhanced the Efficacy of Chemotherapeutic Agents in ABCB1- and ABCG2-Overexpressing Cells In Vitro, In Vivo, and Ex Vivo, Mol. Cancer Ther. 8 (2016) 1845–1858, https://doi.org/10.1158/1535-7163.MCT-15-0939.
[35] S. Peters, S. Zimmermann, A.A. Adjei, Oral epidermal growth factor receptor tyrosine kinase inhibitors for the treatment of non-small cell lung cancer: comparative pharmacokinetics and drug-drug interactions, Cancer Treat. Rev. 8 (2014) 917–926, https://doi.org/10.1016/j.ctrv.2014.06.010.
[36] M. Visentin, P. Biason, G. Toffoli, Drug interactions among the epidermal growth factor receptor inhibitors, other biologics and cytotoxic agents, Pharmacol. Ther. 1 (2010) 82–90, https://doi.org/10.1016/j.pharmthera.2010.05.005.
[37] S. Durmus, R.W. Sparidans, E. Wagenaar, et al., Oral availability and brain penetration of the B-RAFV600E inhibitor vemurafenib can be enhanced by the P-GLYCOprotein (ABCB1) and breast cancer resistance protein (ABCG2) inhibitor elacridar, Mol. Pharm. 11 (2012) 3236–3245, https://doi.org/10.1021/mp3003144.
[38] A.H. Schinkel, U. Mayer, E. Wagenaar, et al., Normal viability and altered pharmacokinetics in mice lacking mdr1-type (drug-transporting) P-glycoproteins, Proc. Natl. Acad. Sci. U. S. A. 8 (1997) 4028–4033.
[39] J.W. Jonker, G. Merino, S. Musters, et al., The breast cancer resistance protein BCRP (ABCG2) concentrates drugs and carcinogenic xenotoxins into milk, Nat. Med. 2 (2005) 127–129, https://doi.org/10.1038/nm1186.
[40] J.W. Jonker, M. Buitelaar, E. Wagenaar, et al., The breast cancer resistance protein protects against a major chlorophyll-derived dietary phototoxin and protoporphyria, Proc. Natl. Acad. Sci. U. S. A. 24 (2002) 15649–15654, https://doi.org/10.1073/pnas.202607599.
[41] R.A. van Waterschoot, J.S. Lagas, E. Wagenaar, et al., Absence of both cytochrome P450 3A and P-glycoprotein dramatically increases docetaxel oral bioavailability and risk of intestinal toxicity, Cancer Res. 23 (2009) 8996–9002, https://doi.org/10.1158/0008-5472.CAN-09-2915.
[42] J.J.M. Rood, M.T.J. van Bussel, J.H.M. Schellens, et al., Liquid chromatography-tandem mass spectrometric assay for the T790M mutant EGFR inhibitor osimertinib (AZD9291) in human plasma, J. Chromatogr. B Analyt. Technol. Biomed. Life Sci. (2016) 80–85, https://doi.org/10.1016/j.jchromb.2016.07.037.
[43] B.D. van Groen, E. van de Steeg, M.G. Mooij, et al., Proteomics of human liver membrane transporters: a focus on fetuses and newborn infants, Eur. J. Pharm. Sci. (2018) 217–227, https://doi.org/10.1016/j.ejps.2018.08.042.
[44] A.K. MacLeod, Huang J.T. Lin, et al., Identification of Novel Pathways of Osimertinib Disposition and Potential Implications for the Outcome of Lung Cancer Therapy, Clin. Cancer Res. 9 (2018) 2138–2147, https://doi.org/10.1158/1078-0432.CCR-17-3555.
[45] W. Li, R.W. Sparidans, Y. Wang, et al., P-glycoprotein and breast cancer resistance protein restrict brigatinib brain accumulation and toxicity, and, alongside CYP3A, limit its oral availability, Pharmacol. Res. (2018) 47–55, https://doi.org/10.1016/j.phrs.2018.09.020.
[46] M. Pesic, J.Z. Markovic, D. Jankovic, et al., Induced resistance in the human non small cell lung carcinoma (NCI-H460) cell line in vitro by anticancer drugs, J. Chemother. 1 (2006) 66–73, https://doi.org/10.1179/joc.2006.18.1.66.
[47] J. Khalifa, A. Amini, S. Popat, et al., Brain metastases from NSCLC: radiation therapy in the era of targeted therapies, J. Thorac. Oncol. 10 (2016) 1627–1643, https://doi.org/10.1016/j.jtho.2016.06.002.
[48] J.S. Lagas, R.A. van Waterschoot, R.W. Sparidans, et al., Breast cancer resistance protein and P-glycoprotein limit sorafenib brain accumulation, Mol. Cancer Ther. 2 (2010) 319–326, https://doi.org/10.1158/1535-7163.mct-09-0663.
[49] R.L. Oostendorp, T. Buckle, J.H. Beijnen, et al., The effect of P-gp (Mdr1a/1b), BCRP (Bcrp1) and P-gp/BCRP inhibitors on the in vivo absorption, distribution, metabolism and excretion of imatinib, Invest. New Drugs 1 (2009) 31–40, https://doi.org/10.1007/s10637-008-9138-z.
[50] S. Agarwal, R. Sane, J.L. Gallardo, et al., Distribution of gefitinib to the brain is limited by P-glycoprotein (ABCB1) and breast cancer resistance protein (ABCG2)-mediated active efflux, J. Pharmacol. Exp. Ther. 1 (2010) 147–155, https://doi.org/10.1124/jpet.110.167601.
[51] A. Kort, S. Durmus, R.W. Sparidans, et al., Brain and Testis Accumulation of Regorafenib is Restricted by Breast Cancer Resistance Protein (BCRP/ABCG2) and P-glycoprotein (P-GP/ABCB1), Pharm. Res. 7 (2015) 2205–2216, https://doi.org/10.1007/s11095-014-1609-7.
[52] A. Kort, S. van Hoppe, R.W. Sparidans, et al., Brain accumulation of ponatinib and its active metabolite, N-desmethyl ponatinib, Is limited by P-glycoprotein (P-GP/ABCB1) and breast cancer resistance protein (BCRP/ABCG2), Mol. Pharm. 10 (2017) 3258–3268, https://doi.org/10.1021/acs.molpharmaceut.7b00257.
[53] S. van Hoppe, R.W. Sparidans, E. Wagenaar, et al., Breast cancer resistance protein (BCRP/ABCG2) and P-glycoprotein (P-gp/ABCB1) transport afatinib and restrict its oral availability and brain accumulation, Pharmacol. Res. (2017) 43–50, https://doi.org/10.1016/j.phrs.2017.01.035.
[54] M.R. Finlay, M. Anderton, S. Ashton, et al., Discovery of a potent and selective EGFR inhibitor (AZD9291) of both sensitizing and T790M resistance mutations that spares the wild type form of the receptor, J. Med. Chem. 20 (2014) 8249–8267, https://doi.org/10.1021/jm500973a.
[55] T. Reungwetwattana, K. Nakagawa, B.C. Cho, et al., CNS response to osimertinib versus standard epidermal growth factor receptor tyrosine kinase inhibitors in patients with untreated EGFR-mutated advanced non-small-cell lung cancer, J. Clin. Oncol. (2018) JCO2018783118, , https://doi.org/10.1200/JCO.2018.78.3118.